URSI GASS 2021, Rome, Italy, 28 August - 4 September 2021

Strategies for Synergistic Use of Microwave and Ultrasound Data For Biomedical Imaging

Pedram Mojabi*, Nozhan Bayat, Puyan Mojabi, and Joe LoVetri
Department of Electrical and Computer Engineering, University of Manitoba, Winnipeg, Manitoba, Canada

Abstract

Different strategies are discussed to synergistically use ultrasound and microwave scattering data to improve image specificity and sensitivity. In particular, we consider methods based on machine learning, statistical measures, regularization, and inhomogeneous background approaches to yield a final image using multimodal ultrasound-microwave imaging.

1 Introduction

In biomedical imaging, ultrasound data can be used to yield qualitative or quantitative information about sound speed, ultrasonic attenuation, compressibility, and density within biological tissues [1, 2]. On the other hand, microwave imaging aims to provide qualitative or quantitative information about the relative complex permittivity of the tissues being imaged [3]. Both types of information are useful for diagnostics. For example, ultrasound imaging typically provides higher spatial resolution as compared to microwave biomedical imaging due to the smaller interrogation wavelengths [4]. On the other hand, the relative complex permittivity information provided by microwave imaging can have a greater contrast between tissues. Therefore, ideally, taking advantage of both modalities should lead to more reliable diagnostics [5]. This paper investigates some approaches that have been proposed for combining both modalities.

The approaches considered herein have been summarized in Fig 1. For completeness the approaches, denoted by Methods 6 and 7 (photoacoustic and thermoacoustic imaging [6]), are included but are not the focus of this paper. These two promising modalities utilize microwaves or lasers to illuminate the object being imaged and then collect the resulting acoustic data. Although these are multiphysics approaches, they are different from the other methods considered herein in the sense that they do not collect both ultrasound and microwave data. Herein, we focus on five different approaches to synergistically use both ultrasound and microwave data. Broadly speaking, these five techniques can be classified under two categories. In the first category, the ultrasound and microwave data are used in parallel to create the final image. In the second category, one dataset is first utilized to create an image. This image, in the form of prior information, is then fed to an inversion algorithm to process the other data set to yield the final image.

2 Methodology

Method 1 in Fig 1 uses a machine learning algorithm to simultaneously process both ultrasound and microwave data to create final tissue-type classification image. On the other hand, Method 2 uses a full-wave inverse scattering approach to simultaneously invert both ultrasound and microwave imaging data wherein the inversions are linked through appropriate regularization terms [7]. Although Method 1 can be very fast, it requires a sufficiently large data set for the training process; however, Method 2 can be computationally expensive, but does not require any training (physics-based inversion). The motivation behind Method 3 is to help the training process in Method 1 by providing an extra piece of training information: a low resolution image. For example, this low resolution image can be obtained via approximations such as fast ray-based approaches or Born approximation. In Method 4, the ultrasound and microwave data are separately inverted to yield ultrasound and microwave property images. For example, these images can be the real and imaginary parts of the relative complex permittivity for microwave imaging, and the compressibility and attenuation images for ultrasound imaging. These images are then given to a machine learning algorithm to predict the final tissue type image [8]. In addition, this machine learning algorithm can provide uncertainty quantification for each pixel in the final tissue type image. To this end, in addition to machine learning approaches, other methods such as the statistical approach used in [9, 10] can also be used.

The first four methods discussed above all belong to the first category in which both ultrasound and microwave data are used in parallel. Alternatively, Method 5 first inverts the ultrasound data to reconstruct ultrasound properties and then uses these reconstructed images to form prior information for the microwave reconstruction algorithm. Subsequently, the microwave reconstruction algorithm uses the microwave data in conjunction with this prior information to reconstruct the final image. Method 5 itself might be implemented in different ways. The simplest mechanism is to use the ultrasound priors as the initial guess for the

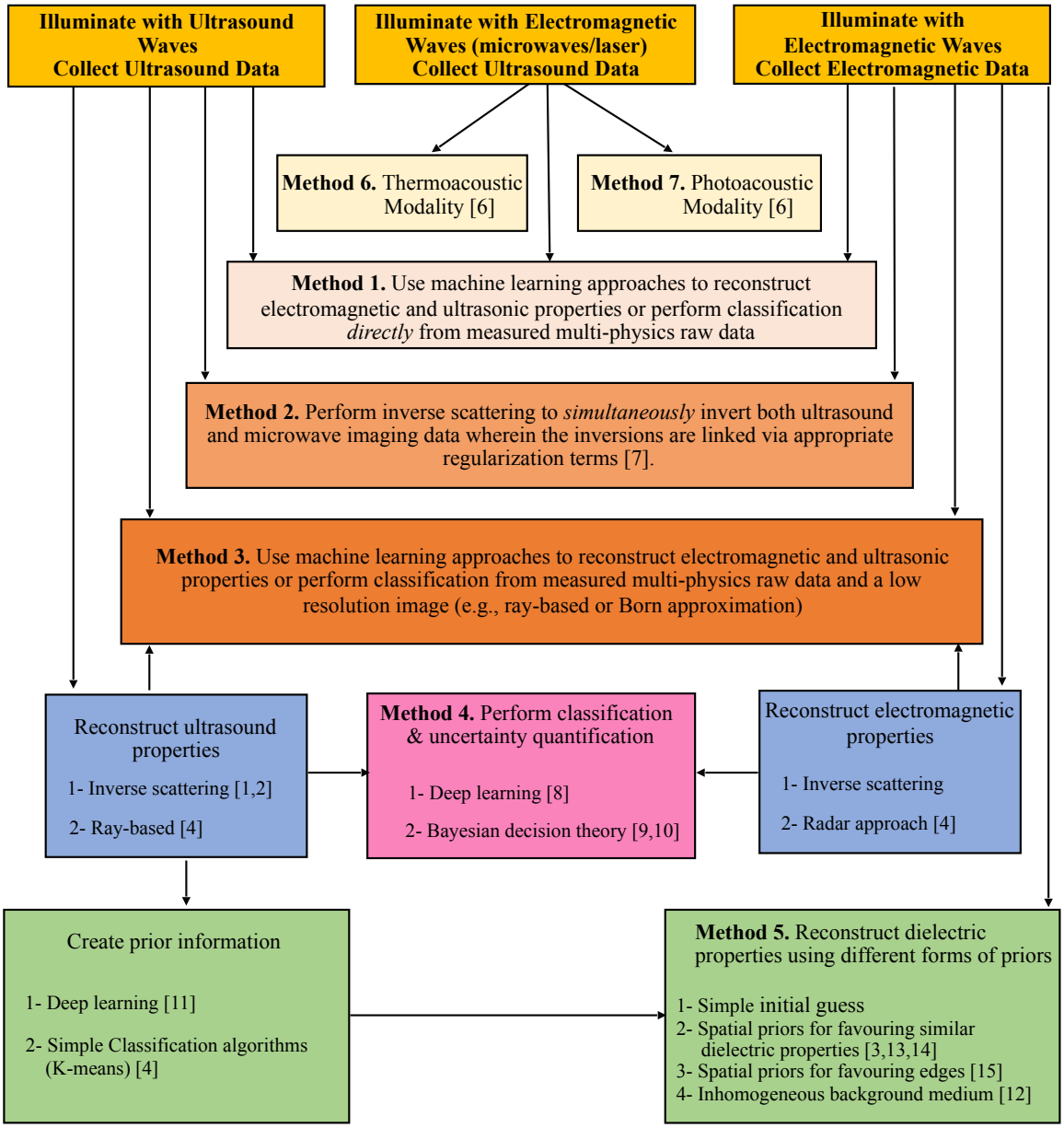

Figure 1. Overview of some joint ultrasound and microwave imaging approaches.

iterative microwave inversion. (This will require permittivity assignment to the ultrasound image which is not trivial.) Alternatively, if permittivity assignment can be done [4,11], we can create an inhomogeneous *numerical* background medium [12] for microwave inversion. The microwave inversion then only needs to reconstruct the contrast with respect to that background medium (e.g., a tumour). Another approach is to use the prior information to create different regions. Then the microwave inversion algorithm will *favour* similar permittivity values in each of these regions [3,13,14]. Finally, we may process the ultrasound image, extract its edges (transition from one tissue type to another), and then provide the microwave reconstruction algorithms with these edge information [15]. As shown in [15], if an edge is missing in the ultrasound image, it might still be recovered during the microwave inversion process.

3 Results

Herein, for brevity, we only show two sample tomographic results; more examples will be presented during the conference. The first example belongs to Method 4 where microwave data are collected at 1, 1.5 and 2 GHz and the ultrasound data are collected from 100, 130 and 160 KHz. Fig 2(a)-(d) shows the real and imaginary parts of the relative complex permittivity and the ultrasonic compressibility and attenuation for our numerical breast phantom. The blind inversion of each of these data sets using the mul-

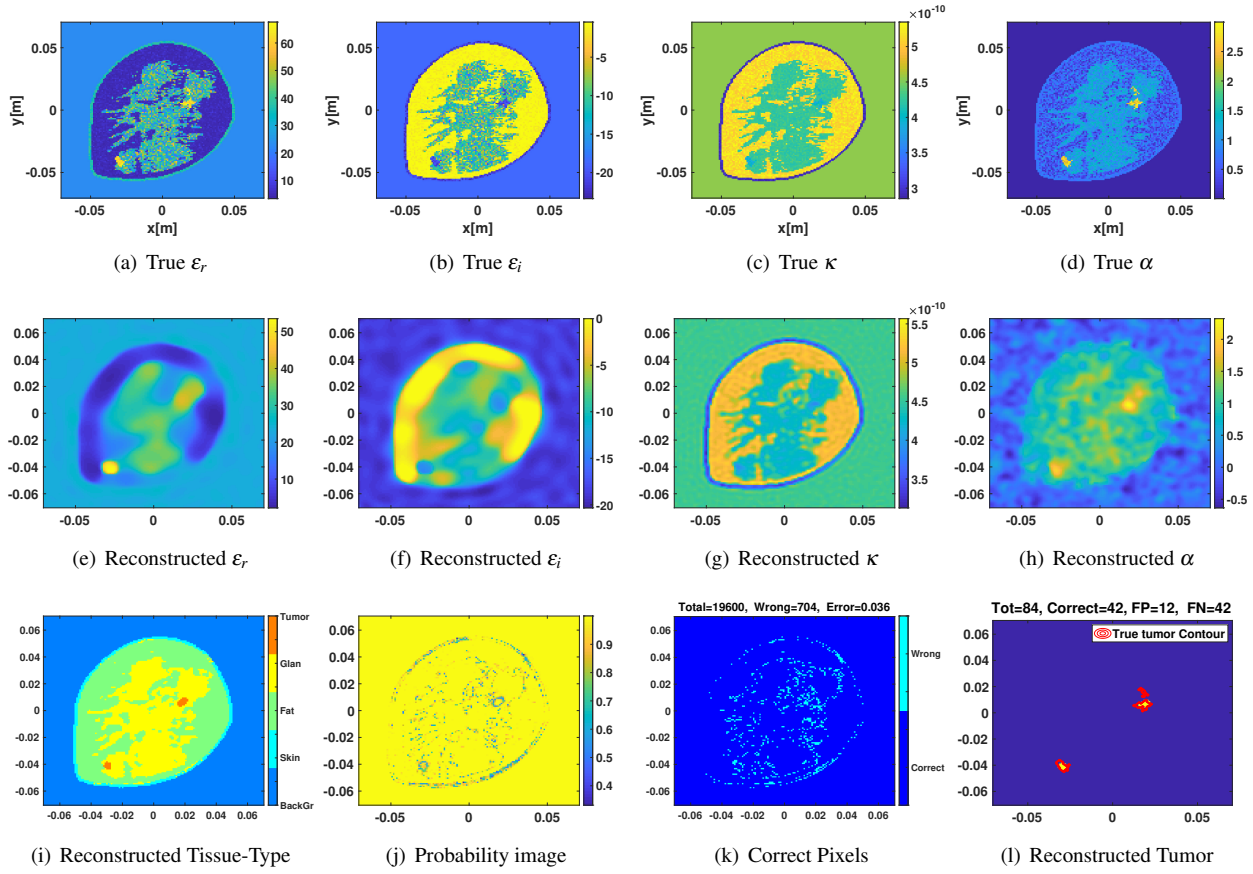

(a) True ε_r (b) True ε_i (c) True κ (d) True α

(e) Reconstructed ε_r (f) Reconstructed ε_i (g) Reconstructed κ (h) Reconstructed α

(i) Reconstructed Tissue-Type (j) Probability image (k) Correct Pixels (l) Reconstructed Tumor

Figure 2. (Top) true relative complex permittivity (ε_r and $j\varepsilon_i$), ultrasonic compressibility κ and attenuation slope α. (Middle) reconstructed properties by blind inversion. (Bottom) reconstructed tissue type image and uncertainty quantification by a CNN approach.

tiplicative regularized Gauss-Newton inversion algorithm (30 and 64 transceivers for microwave and ultrasound data respectively) is shown in the second row of this figure. We have given these four reconstructed images to a convolutional neural network (CNN) that has been trained for this application. The details of this CNN can be found in [8]. The final output of this CNN is a tissue-type image shown in Fig 2(i), along with an uncertainty quantification image shown in Fig 2(j). We have also provided the information about the pixels whose tissue types have been correctly identified by the CNN in Fig 2(k). Finally, we can see the true contour of tumours along with the recovered ones in Fig 2(l). As can be seen, one small tumour region has been missed by the CNN (the pixel-based false- and true-positive metrics are provided at the top of the figure). This is expected for tumors with small ultrasound and microwave scattering signatures for a given signal to noise ratio of the data.

Finally, let us consider a single-frequency microwave (1 GHz) example for Method 5. The true numerical tissue type breast phantom considered for this example is shown in Fig 3(a), which is the same numerical phantom used in [11]. The blind microwave reconstruction of the relative complex permittivity is shown in Fig 3(b)-(c). Then, we perform ultrasound Born inversion and provide the microwave reconstruction algorithm with the prior information (in this case, edge information [15]) extracted from the ultrasound image[1], yielding the reconstruction shown in Fig 3(d)-(e). As can be seen, the tumours are more clearly visible in the new reconstruction.

4 Conclusions

We have overviewed and categorized several approaches that synergistically utilize both microwave and ultrasound scattering data to yield one final property image or a tissue classification image. Two methods have been considered herein, and examples using the other approaches will be presented at the conference. The final choice regarding which method to choose depends on several factors which can only be better understood once these methods are applied and tested with data obtained using real experimental systems. Registration errors between modalities need to be taken into account and minimized. This can only be properly studied using systems capable of obtaining both ultra-

[1] In contrast to [16], in which we use full-wave ultrasound inversion to create the spatial priors, herein we have used the ultrasound Born approximation in conjunction with a CNN [11] to create the spatial priors.

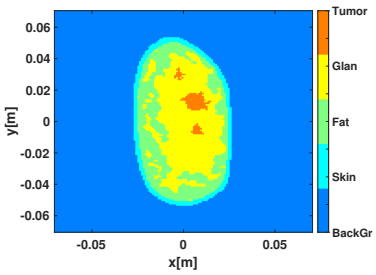

(a) True tissue-type image

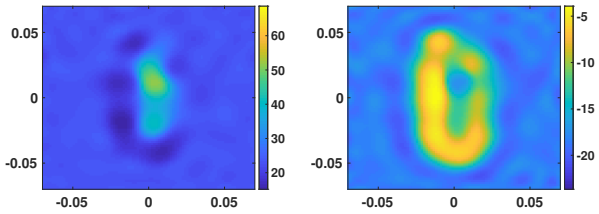

(b) Reconstructed ε_r (Blind) (c) Reconstructed ε_i (Blind)

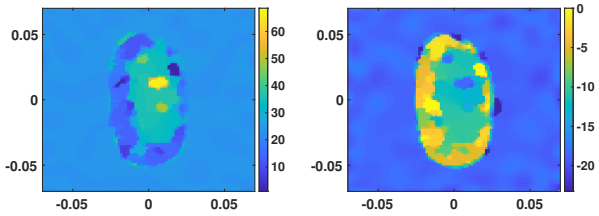

(d) Reconstructed ε_r (edge priors) (e) Reconstructed ε_i (edge priors)

Figure 3. (a) True tissue-type image; (b)-(c) the reconstructed relative complex permittivity using blind microwave inversion. (d)-(e) reconstructed relative complex permittivity using microwave inversion with spatial priors.

sonic and microwave data. The answer to such questions help us determine an appropriate method for a given scenario and application.

References

[1] P. Mojabi and J. LoVetri, "Ultrasound tomography for simultaneous reconstruction of acoustic density, attenuation, and compressibility profiles," *J. Acoust. Soc. Amer*, vol. 137, p. 1813, 04 2015.

[2] P. Mojabi and J. LoVetri, "Evaluation of balanced ultrasound breast imaging under three density profile assumptions," *IEEE Trans. Comput. Imag.*, vol. 3, no. 4, pp. 864–875, 2017.

[3] L. M. Neira, B. D. Van Veen, and S. C. Hagness, "High-resolution microwave breast imaging using a 3-D inverse scattering algorithm with a variable-strength spatial prior constraint," *IEEE Trans. Antennas Propag.*, vol. 65, no. 11, pp. 6002–6014, 2017.

[4] M. Omer, P. Mojabi, D. Kurrant, J. LoVetri, and E. Fear, "Proof-of-concept of the incorporation of ultrasound-derived structural information into microwave radar imaging," *IEEE J. Multiscale Multiphys. Comput. Techn.*, vol. 3, pp. 129–139, 2018.

[5] H. Jiang et al., "Ultrasound-guided microwave imaging of breast cancer: Tissue phantom and pilot clinical experiments," *Med. Phys.*, vol. 32, no. 8, pp. 2528–2535, 2005.

[6] M. Pramanik, G. Ku, C. Li, and L. V. Wang, "Design and evaluation of a novel breast cancer detection system combining both thermoacoustic (TA) and photoacoustic (PA) tomography," *Medical Physics*, vol. 35, no. 6Part1, pp. 2218–2223, 2008.

[7] X. Song, M. Li, F. Yang, S. Xu, and A. Abubakar, "Three-Dimensional Joint Inversion of EM and Acoustic Data Based on Contrast Source Inversion," *IEEE J. Multiscale Multiphys. Comput. Techn.*, vol. 5, pp. 28–36, 2020.

[8] P. Mojabi, V. Khoshdel, and J. Lovetri, "Tissue-type classification with uncertainty quantification of microwave and ultrasound breast imaging: A deep learning approach," *IEEE Access*, vol. 8, pp. 182 092–182 104, 2020.

[9] P. Mojabi and J. LoVetri, "Composite tissue-type and probability image for ultrasound and microwave tomography," *IEEE J. Multiscale Multiphys. Comput. Techn.*, vol. 1, pp. 26–35, 2016.

[10] ——, "Experimental evaluation of composite tissue-type ultrasound and microwave imaging," *IEEE J. Multiscale Multiphys. Comput. Techn.*, vol. 4, pp. 119–132, 2019.

[11] P. Mojabi et al., "CNN for compressibility to permittivity mapping for combined ultrasound-microwave breast imaging," *Submitted to IEEE J. Multiscale Multiphys. Comput. Techn.*, 2020.

[12] N. Abdollahi, D. Kurrant, P. Mojabi, M. Omer, E. Fear, and J. LoVetri, "Incorporation of ultrasonic prior information for improving quantitative microwave imaging of breast," *IEEE J. Multiscale Multiphys. Comput. Techn.*, vol. 4, pp. 98–110, 2019.

[13] P. Meaney et al., "Integration of microwave tomography with magnetic resonance for improved breast imaging," *Medical Physics*, vol. 40, no. 10, 2013.

[14] N. Bayat and P. Mojabi, "Incorporating spatial priors in microwave imaging via multiplicative regularization," *IEEE Trans. Antennas Propag.*, vol. 68, no. 2, pp. 1107–1118, 2020.

[15] ——, "A multiplicative regularizer augmented with spatial priors for microwave imaging," *IEEE Trans. Antennas Propag.*, vol. 69, no. 1, pp. 606–611, 2021.

[16] N. Bayat, P. Mojabi, J. LoVetri, and P. Mojabi, "On microwave breast imaging with ultrasound spatial priors," *URSI-GASS Conference*, pp. 1–4, 2020.